

Multi-wavelength fibril dynamics and oscillations above sunspot – I. morphological signature

Emanuel Sungging Mumpuni^{1,2}, Dhani Herdiwijaya¹, Mitra Djamal³ and
Thomas Djamaluddin²

¹ Graduate Program in Astronomy, Faculty of Mathematics and Natural Sciences, Bandung
Institute of Technology, Gedung CAS Lt. 6 ITB, Jl. Ganesha 10 Bandung 40132, Indonesia;
nggieng@students.itb.ac.id

² Space Science Center, LAPAN, Indonesia

³ Graduate Program in Physics, Faculty of Mathematics and Natural Sciences, Bandung Institute
of Technology, Department of Physics, Jl. Ganesha 10 Bandung 40132, Indonesia

Received 2014 October 19; accepted 2015 March 27

Abstract In this work we selected one particular fibril from a high resolution observation of the solar chromosphere with the Dutch Open Telescope, and tried to obtain a broad picture of the intricate mechanism that might be operating in the multiple layers of the solar atmosphere visible in high cadence multi-wavelength observations. We analyzed the changing fibril pattern using multi-wavelength tomography, which consists of both the $H\alpha$ line center and the blue wing, Doppler signal, Ca II H, and the G-band. We have found that the intermittent ejected material through the fibril from Doppler images has clearly shown an oscillation mode, as seen in the $H\alpha$ blue wing. The oscillations in the umbrae and penumbrae magnetic field lines that are above the sunspot cause a broadening and the area forms a ring shape from 3 to 15 minute oscillations as a function of height. These made a distinct boundary between the umbrae and penumbrae which suggests a comb structure, and indicates that the oscillations could propagate along the inclined magnetic flux tubes from below. The 3 minute oscillations strongly appeared in the broadly inclined penumbrae magnetic field lines and showed a clear light bridge. The well known 5 minute oscillations were dominant in the umbrae-penumbrae region boundary. The long 7 minute oscillations were transparent in the $H\alpha$ blue wing, as well as the 10 and 15 minute oscillations. They were concentrated in the inner-penumbrae, as seen in the $H\alpha$ line center. From these findings we propose that the fibril acts as a fabric for interaction between the layers, as well as related activities around the active region under investigation.

Key words: Sun: chromosphere — Sun: oscillations — Sun: sunspots

1 INTRODUCTION

Researchers do not yet have a complete picture of the complex coupled interactions between the photosphere, chromosphere and corona. The structure of the photosphere is relatively well understood but not that of the chromosphere, in particular the dynamics associated with energy and mass

transport in a fibril, as is discussed in detail in Rutten (2012). Instead of mass transfer, i.e. downflow and upflow from photosphere to chromosphere and corona, a variety of oscillation modes have been observed, such as 3 minute oscillations, 5 minute oscillations, 7 minute oscillations, etc. They act as one physical unit that accomplishes mass and energy transfer from the photospheric to chromospheric layers, and vice-versa.

Recently, an image sequence with high spatial and temporal resolution, acquired by ground and space based observations, confirmed and revealed the number of oscillation modes (Nagashima et al. 2007; Reznikova & Sibasaki 2012; Jess et al. 2012). Naturally, a disturbance or instability in magnetic structures will trigger such oscillations. Observations of sunspot oscillations have been taken for almost four decades (Beckers & Tallant 1969; Bogdan & Judge 2006 and references therein). The 5 minute oscillations (Leighton et al. 1962) that predominantly occur above the sunspot in the photosphere have also been relatively well studied. Their amplitudes decrease with height, and they can hardly be detected in the upper chromosphere and transition region. Lites (1992) summarized the 3 minute oscillations and drew the possible conclusion that the resonance is a response from many oscillation modes located below and results in driving the wave modes.

Moreover, Centeno et al. (2006) also suggested propagating shock waves in umbrae regions. The 3 minute oscillations could be due to a complex interaction of many processes, especially magneto-acoustic mode conversion and intrinsic reduced acoustic emissivity in strong magnetic fields (Stangalini et al. 2012). So, it was clear that the oscillations and wave propagation are the key processes for carrying energy and mass through different atmospheric layers, before dissipating them into other modes.

By analyzing the oscillations and wave propagation, we can investigate the physical mechanism leading to stratification and the dynamics related to different magnetized atmospheric structures. The conversion into thermal heating, e.g. coronal heating, is a major question and has become one of the most challenging research areas in solar physics. The magnetic field lines are mostly believed to play a crucial role. However, there were still many unanswered problems related to these oscillation modes and their connection with other dynamic structures like fibrils and light bridges (LBs). This work will study the chromospheric dynamics and how they are related to the photosphere by studying sunspot umbrae, penumbrae and a fibril from a sequence of high resolution multiwavelength images. The results from the Dutch Open Telescope (DOT) are analyzed as a diagnostic tool for tomography of the Sun (Rutten et al. 2004). The selection of $H\alpha$ images as the primary tool acts as a much more complete proxy to delineate chromospheric magnetic topology which consists of the mass flow along fibrils (Rutten 2007). In this study we found a morphological signature that indicates mass motion which may be related to wave propagation.

To study the dynamics of each particular layer of the atmosphere, we use the tomographic image analysis method for each particular feature, such as the G -band, Ca II H line and $H\alpha$ which act as tracers for activity in the photosphere, the lower chromosphere, and the upper chromosphere, respectively. We will also address several oscillation modes of umbrae and penumbrae by simultaneously using multi-wavelength observations that form a time series. We believe that this powerful technique can most sensitively detect wave propagation.

In Section 2, we briefly describe the DOT observations and the data reduction procedures. Some interesting results on the fibril mass transfer and oscillations are reported in Section 3. Discussions on the fibril and LB oscillations are given in Section 4. Conclusions are drawn in Section 5.

2 DATA AND ANALYSIS

The sunspot of NOAA Active Region (AR) 10789 (N17W23) that was located close to the disk center on 2005 July 13 was selected for this study (Fig. 1). This AR had a simple bipolar structure with magnetic and McIntosh classifications of beta and Eao, respectively. There were no flares reported within three days before or after the date of observation. A series of high angular resolution images of

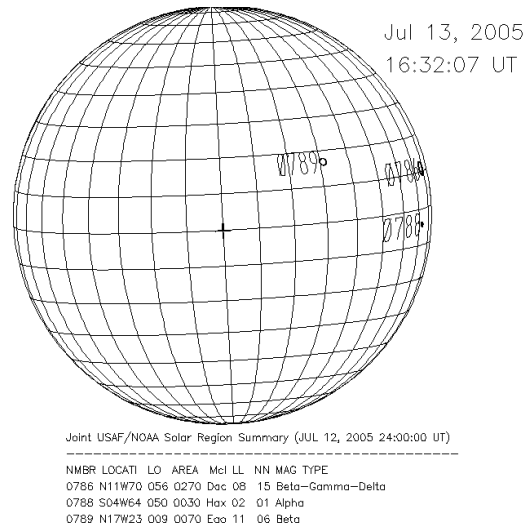


Fig. 1 The position of AR 10789. This region has McIntosh classification Eao and magnetic type beta.

a sunspot at AR 10789 on 2005 July 13 has been carefully filtered and aligned from the observation results of the DOT. The multiple wavelength observations from the Ca II H line, *G*-band, H α line center, H α blue wing and H α Doppler signal images were taken simultaneously at that time.

The capabilities of the multi-wavelength re-imaging system of the DOT, as well as the associated instrumentations, speckle acquisition and reconstruction have been discussed by Rutten et al. (2004).

The data have already been speckle reconstructed from the observational run on 07:49 – 10:35 UT to give a resolution of $0.071'' \text{ pix}^{-1}$. There are 332 images in total with a time cadence of 30 s for each band. An interesting feature in the form of an LB appeared across the fairly round main umbrae, instead of being a long fibril across the penumbra (Fig. 2). To investigate the dynamics of the region, we selected a particular area of interest and studied the Doppler signal images. We constructed the difference image from Doppler signals which would show a particular feature with a fibrillar pattern in which we are interested. Then, we manually determined a clear and persistent feature for the region under investigation, as shown in Figure 2.

3 RESULTS

3.1 Fibril Mass Transfer

Figure 3 illustrates the fibril under investigation (region (a), upper circular sector) from the H α line center, and lower circular sector as a comparison (region (b)). The angle subtended by the sector is 10 degrees. The right panels show the integrated cross-section of the upper (a) and lower (b) circular sectors. The radius of the umbrae regions is 52 pixels and the penumbrae region extends to 105 pixels. The selection of the circular sector is based on the assumption that the magnetic field will be stronger inside the umbrae region compared to outside the region. Using this method, we can deduce that there was a fibrillar pattern under region (a), which has a length of about 150 pixels. The normalized integrated intensity (total integrated intensity divided by the number of pixels in the circle) of region (a) was higher in the umbrae region than in region (b), but it was also about the same in the penumbrae area. So, we will further analyze region (a).

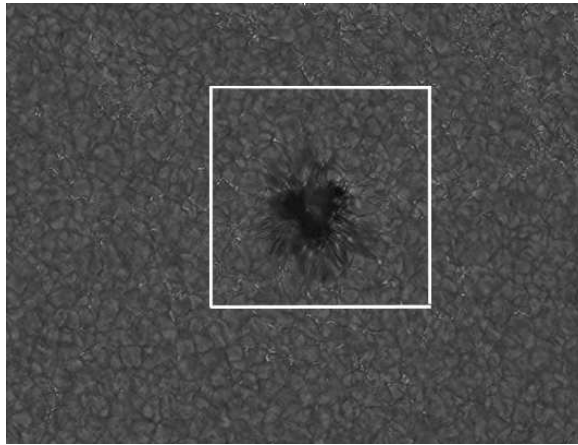


Fig. 2 NOAA AR 10789 observed on 2005 July 13 from the G -band images. The white box is the selected area that is being studied with multi-wavelength analysis. The picture size is $76.25'' \times 57.79''$ with resolution $0.071'' \text{ pix}^{-1}$.

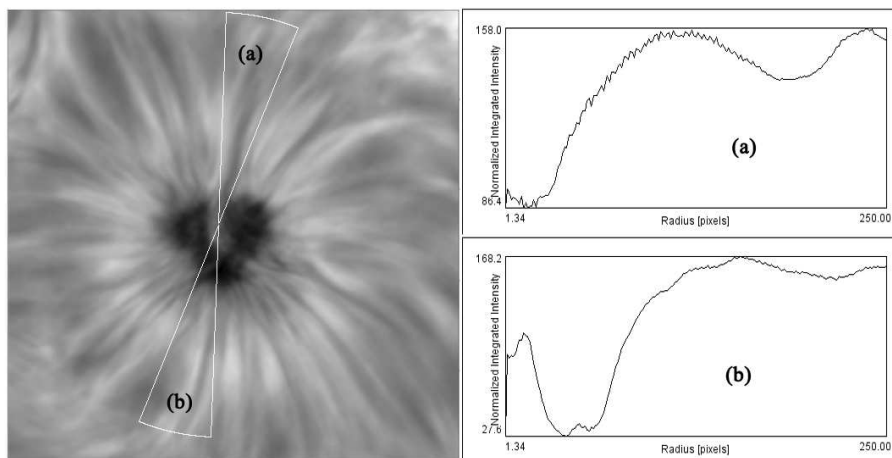


Fig. 3 In the $H\alpha$ line center image, the fibril under investigation is marked in the upper circular sector (a), while the opposite lower circular sector is selected as a comparison (b). The graphs show the integrated cross-section of the area under investigation, with the top panel representing the fibril area (a) and the bottom panel signifying the opposite direction (b).

After selecting the area in region (a), we then follow how the chosen fibrillar pattern changes over time by slicing the central part of the selected region, to see how the mass transfer changed sequentially over time. We argue that the pattern of mass transfer from this morphological signature is related to filamentary structures with filling mass proposed by Rutten (2006). The same procedures were conducted for other wavelengths including the $H\alpha$ blue wing, $H\alpha$ line center, Ca II H and G -band. From the $H\alpha$ Doppler signal, it appeared that there was a pattern of alternating features, right in the middle of the picture. This is marked with the white rectangle with a width of 7 pixels, as

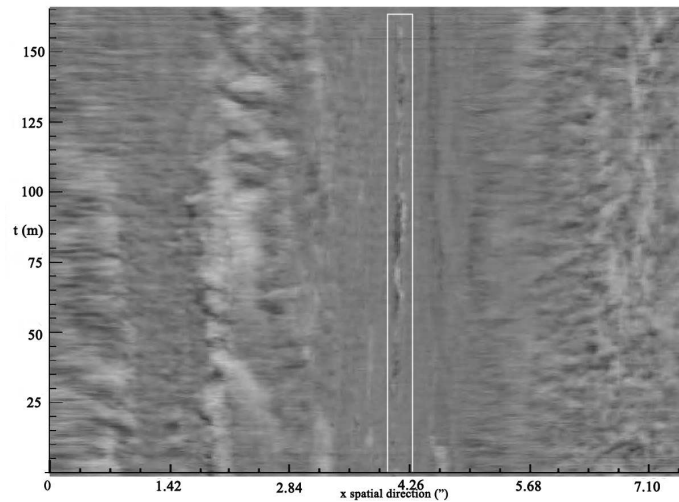


Fig. 4 Time slice in the Doppler signal image of a selected region where the x -axis represents the x direction and the y -axis represents the time slice of 332 images. The area under investigation is in the white rectangle. The center of the rectangle is the middle of the circular sector (a) in Figure 3, with the direction of spatial direction along the x direction, and bottom to top corresponds to propagation in time.

shown in Figure 4. The results of the area profile for each band are shown in Figure 5. Each time marker is equal to 30 s.

We follow the time propagation in detail using data from the whole slice. The upflow mass transfer was clearly seen from the photosphere to the chromosphere layers, see the solid line on the left in Figure 5. However, the downflow also occurred from the chromosphere, as indicated by the dashed line on the right in the same figure.

In the fibril, we find that upward motion predominantly occurred from below and aligned with the magnetic field, as seen in G -band and Ca II H, respectively. During that short period, the collection of material from below streamed to the upper or lower layers and changed the pattern of oscillation in the H α Doppler signal and H α blue wing. It can be seen that the mass transfer flow is not a continuous pattern but rather displayed rapid changes in less than 30 s, especially in the upper level which suggested that, geometrically, the fibril has a tree-like structure.

3.2 Umbrae, Penumbrae and Fibril Oscillations

In order to estimate the strength of an oscillation, the squared amplitude or power, which in our case is the “power-map,” was computed from the Fourier transform (White & Athay 1979). Then we created 2-D power-maps of several periods on multi-wavelength bands (G -band, Ca II H α , H α line center and H α blue wing) at 3, 5, 7, 10 and 15 minutes, and the H α Doppler signal as shown in Figure 6. McAteer et al. (2002) showed that several spectral signatures were detected near 7, 10 and 15 minutes. The method for the power-map was discussed in Krijger et al. (2001). Since the H α blue wing is the best proxy of a magnetometer that can locate and spatially track extended magnetic elements, this line is the “chromospheric” line that can be used as a photospheric diagnostic (Leenaarts et al. 2006). This work will address relationships between oscillations in the umbrae, penumbrae and the fibril which are important for studying the relationship between the fibril and the sunspot (Chae et al. 2014).

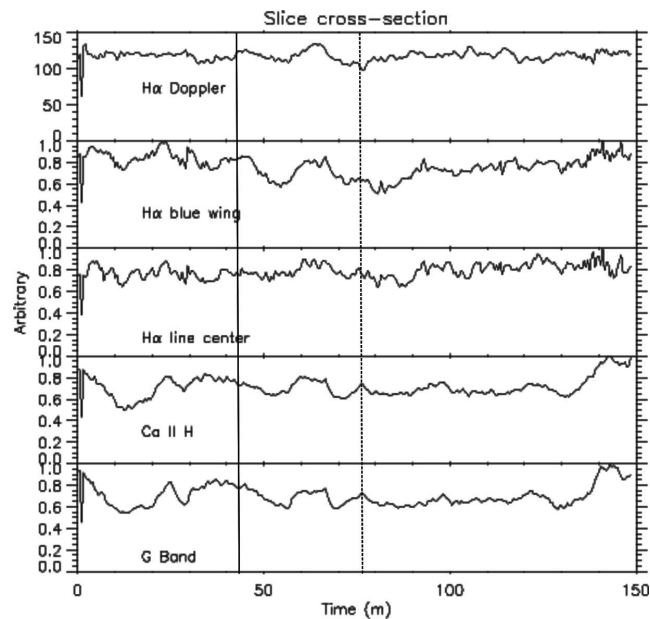


Fig. 5 Cross-section of the time slice of various multi-wavelength images. From top to bottom: $H\alpha$ Doppler signal, blue wing and line center, Ca II H and G-band. The x axis is the time direction of the slice and y is an arbitrary intensity scale for the 332 images.

The Doppler signal indicates that there was an oscillation pattern that appeared during several moments in between material loadings. To understand how the material flows along fibrils, we need to compare oscillatory signatures, both radial and along the fibril.

To examine the layer by layer dynamics in the atmosphere, we use the power-maps from the multi-wavelength observations. The 3 minute oscillations were mainly observed in the chromosphere, 5 minute oscillations were predominantly photospheric, and the longer period cases were sunspot oscillations that were described by Staude (1999) and Bogdan (2000). McAteer et al. (2002) suggested the presence of multiple peaks in the power spectrum with periods in the 4–15 minute range.

For each region (a) indicated in Figure 3, we follow the pattern of the fibril under investigation as shown in Figure 6. From visual inspection in Figure 6, we found that the fibrillar pattern appears strongly in the $H\alpha$ blue wing, in particular with a reversal pattern (bright) in the 15 minute oscillations (6th column, 2nd row).

However, for a larger picture of the active region, we found that for this $H\alpha$ blue wing, there is also a pattern of brightening in the umbra region, in the 3 minute oscillations (2nd column, 2nd row). The same brightening pattern also appeared in the $H\alpha$ line center (2nd column, 3rd row) and the $H\alpha$ Doppler signal (2nd column, 1st row) in Figure 6.

It was seen that the oscillations above the sunspot in the umbrae show a dark and bright ring shape as a function of height and distinctively divide the umbrae from the penumbrae which suggests a comb structure, and indicates that the oscillation could propagate along the inclined magnetic flux tubes from below.

Figures 7 to 11 show the radius profile of the fibril in region (a) of Figure 3 for each mode of power for each wavelength, with Doppler signal as a comparison on the lower panel for each mode.

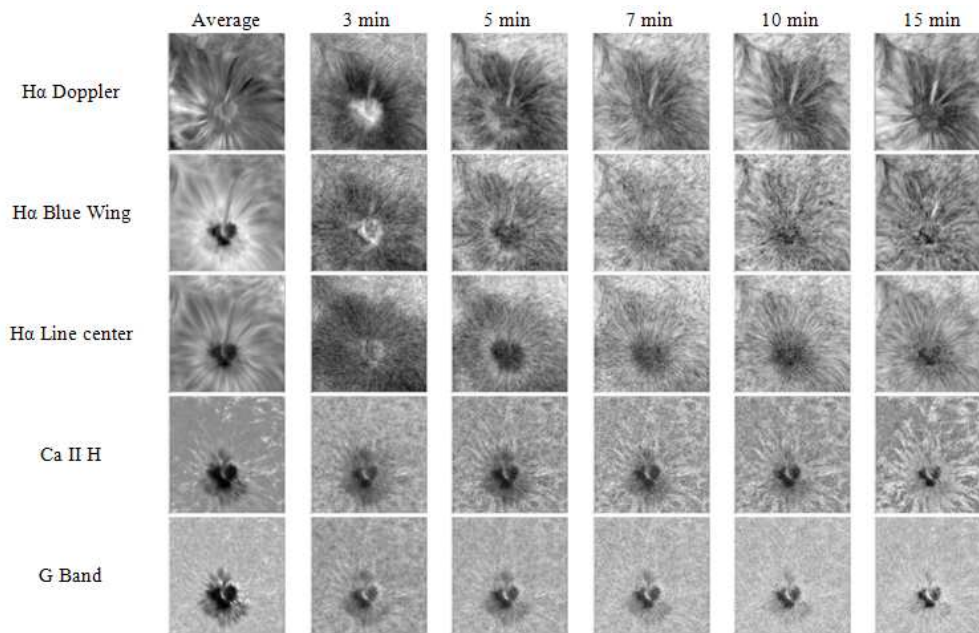


Fig. 6 Comparison of average (1st column) with power-maps from 3, 5, 7, 10 and 15 minutes (second to sixth column respectively), in several wavelengths: $H\alpha$ Doppler (1st row), $H\alpha$ blue wing, center line, Ca II H and G -band (second to fifth row respectively). The size of the window is 512×512 pixels.

The arrow in each figure from Figure 7 to Figure 11 marks the separation between the umbrae and penumbrae.

3.2.1 3 minute Oscillations

In Figure 6, the 3 minute oscillations strongly appeared in the bright area of the $H\alpha$ blue wing due to the broad inclined penumbrae magnetic field lines in which magneto-acoustic waves could be channeled along them. It seems that the 3 minute oscillations could also have a broader area from the photosphere to the chromosphere, even through the solar coronal fan (Jess et al. 2012).

Moreover, the 3 minute oscillations trace a clear boundary between the LB and ejected material, as clearly seen in the $H\alpha$ line center and $H\alpha$ blue wing. The brightening in the umbrae region, as seen in Figure 6 corresponds to the downflow motion as shown in its profile in Figure 7. The downflow patterns happened in the inner and outer bright rings. The penumbral and fibril region showed upflow and downflow patterns, respectively. The 3 minute responses were distinctly different in the photosphere and chromosphere, particularly in the penumbrae region which may be due to the magnetic field strength and its inclination (Schad et al. 2013).

The dynamics indicated by the Ca II H line agree with those of the G -band in the penumbrae region. Our results demonstrate that the dynamics associated with the umbrae-penumbrae boundary show a more complex picture and are crucial for modeling the physical mechanisms. From the $H\alpha$ Doppler signal, the inner umbrae flow shows an opposite direction in the 3 minute case compared to cases from 5 minutes to 15 minutes, which indicates that 3 minute oscillations might play an important role in downward mass motion for the fibril. There was a strong enhancement on the

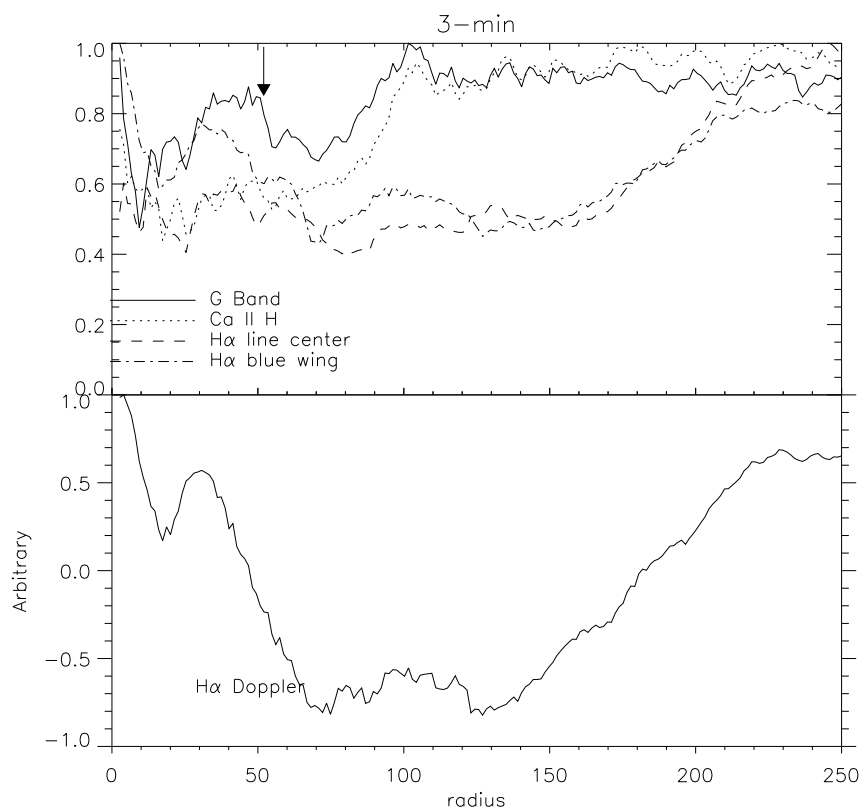


Fig. 7 Integrated profile for the 3 minute mode in the circular sector of the fibril in region (a) as described in Fig. 3 for each wavelength, with a comparison of the Doppler signal in the lower panel. The arrow marks the umbrae region for the smaller radius and the penumbrae region for the larger radius.

Doppler signal in the 3 minute oscillations that might cause an enhancement in the chromospheric line of H α and might lead to umbral flash (Roupe van der Voort et al. 2003).

In the quiet region, that had a radius of more than 190 pixels, there was no difference among indicator lines for the 3 minute oscillations in which they gradually reverse to a downward motion.

3.2.2 5 Minute Oscillations

The well known 5 minute oscillations (Leighton et al. 1962) were dominant in the outer umbrae region near the boundary of umbrae-penumbrae, as in the H α blue wing, which suggests a comb structure that is predominantly in the downward motion, see Figure 8. It was related to the downward motion, in contrast with the inner umbrae. In the boundary between the umbrae and penumbrae, there was a so-called “terminal region” that was evident from the Doppler shift which represents the same response of photospheric and chromospheric indicator lines. The characteristics in the penumbrae and quiet region are the same as 3 minute oscillations. Both oscillation modes were sensitive to magnetic field strength and its inclination, as well as mass motion flow.

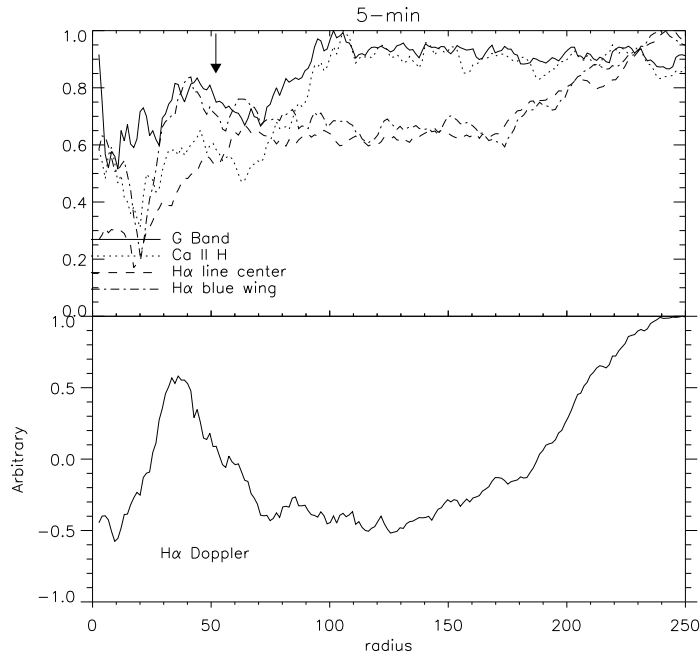


Fig. 8 Integrated profile for the 5 minute mode in the circular sector of the fibril in region (a) as described in Fig. 3 for each wavelength, with a comparison of the Doppler signal in the lower panel. The arrow marks the umbrae region for the smaller radius and the penumbrae region for the larger radius.

3.2.3 7 Minute Oscillations

In Figure 9, the 7 minute oscillations have the same pattern in the H α blue wing and G-band in all areas which means that these oscillations were not too sensitive in the photosphere, chromosphere, penumbrae and quiet area. The difference in the umbrae magnetic field and inclination may cause this kind of oscillation. Some downflow motion still occurred in the umbrae region. The downflow was more dominant in the larger terminal region of the radius, but the inner penumbrae showed an upward mass transfer. Moreover, the penumbrae region did not show significant downward flow.

3.2.4 10-Minute Oscillations

In Figure 10, there was no large fluctuation in flow along the near boundary of umbrae-penumbrae to the boundary of the penumbrae-quiet area. All chromospheric lines had the same pattern. This suggests that 10 minute oscillations excite the chromospheric layer with a relatively small magnetic field strength and inclination.

3.2.5 15-Minute Oscillations

In Figure 11, there was an upward motion in the inner umbrae and the boundary of the penumbrae-quiet region which influences the intensity of this oscillation. The H α line center was damped compared to the Ca II H. Except in the inner umbrae, the intensity of all lines showed almost the same

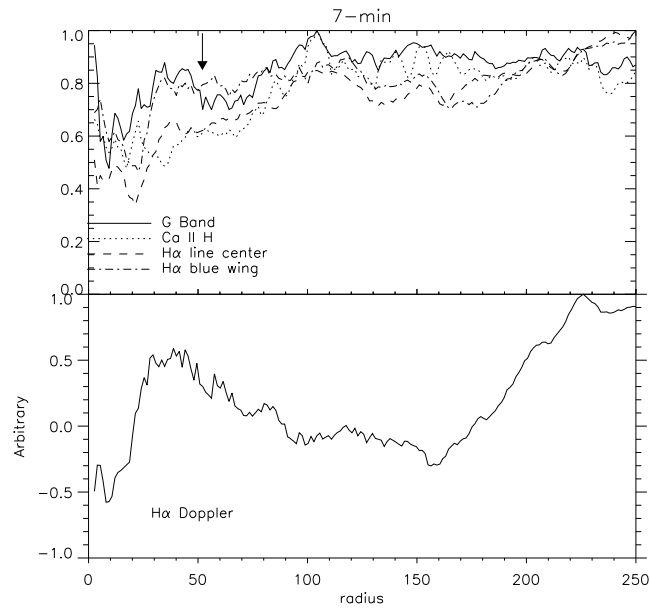


Fig. 9 Integrated profile for the 7 minute mode in the circular sector of the fibril in region (a) as described in Fig. 3 for each wavelength, with a comparison of the Doppler signal in the lower panel. The arrow marks the umbrae region for the smaller radius and the penumbrae region for the larger radius.

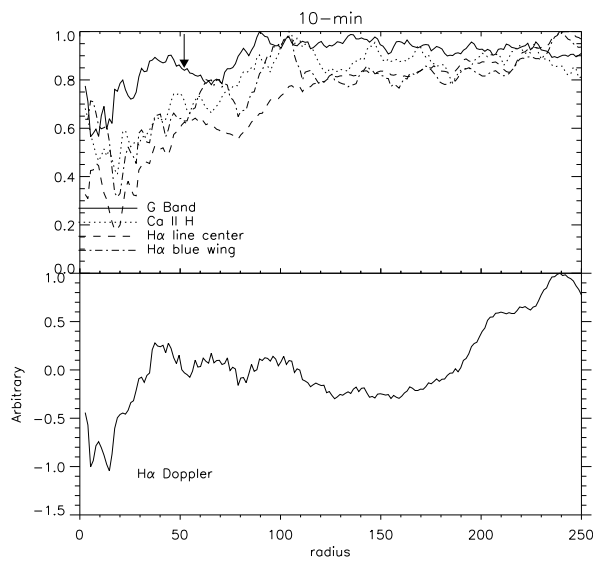


Fig. 10 Integrated profile for the 10 minute mode in the circular sector of the fibril in region (a) as described in Fig. 3 for each wavelength, with a comparison of the Doppler signal in the lower panel. The arrow marks the umbrae region for the smaller radius and the penumbrae region for the larger radius.

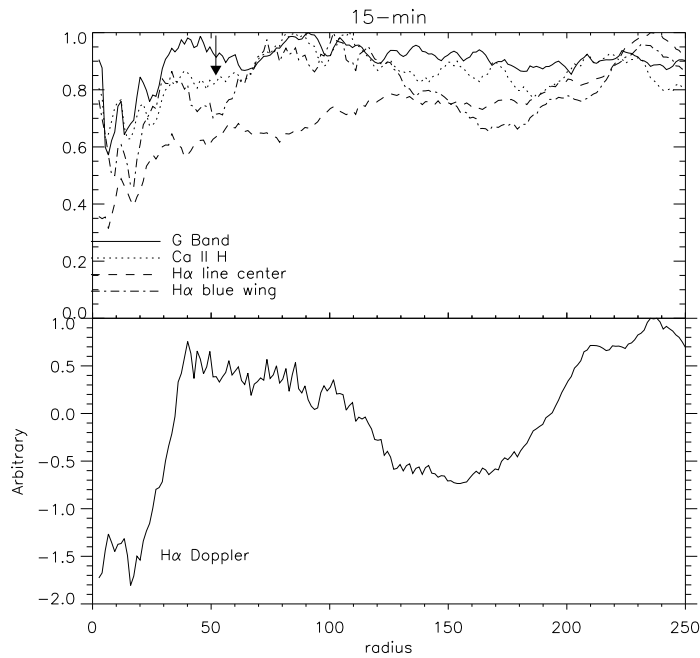


Fig. 11 Integrated profile for the 15 minute mode in the circular sector of the fibril in region (a) as described in Fig. 3 for each wavelength, with a comparison of the Doppler signal in the lower panel. The arrow marks the umbrae region for the smaller radius and the penumbrae region for the larger radius.

value. As for 7 minute oscillations, this mode was not significantly influenced by changes in the magnetic field.

3.3 Root of the Fibril

We tried to compare the result with TRACE data (Handy et al. 1999), particularly 1600 \AA , where Krijger et al. (2001) argue that the radiation is from the “temperature minimum region,” based on the work of Vernazza et al. (1981). There were 18 data sets available for the window of the same observation, with 9 minute cadences of 768×768 pixels for 1600 \AA and $0.5'' \text{ pix}^{-1}$. We made a power-map for the 15 minute case of 1600 \AA , as shown in Figure 12 and manually aligned the data with other data from similar regions.

From Figure 12, it can be seen that there was no significant feature that appeared in the 15 minute case of 1600 \AA , except for the inner umbrae. Since the “temperature minimum region” formed below, near the photosphere, at $h = 500 \text{ km}$ above continuum optical depth $\tau_5 = 1$ at $\lambda = 5000 \text{ \AA}$ and defines the transition from the photosphere to chromosphere (Krijger et al. 2001; Vernazza et al. 1981), it appeared that the root of the fibril formed somewhere else.

4 DISCUSSION

We propose a picture describing how the photosphere is related to the chromosphere and how the fibril acts as a fabric in the interaction between layers, as shown in Figure 13. As seen in Figure 13, even for the dominant 5 minute case, there were various frequencies occurring near the photosphere.

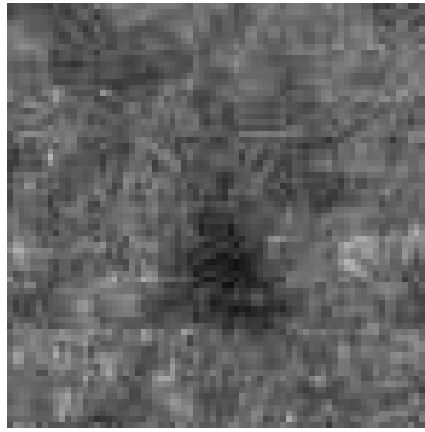


Fig. 12 The power-map for the 15 minute case at 1600 Å, resized on spatial resolution with other power-map pictures of Fig. 6.

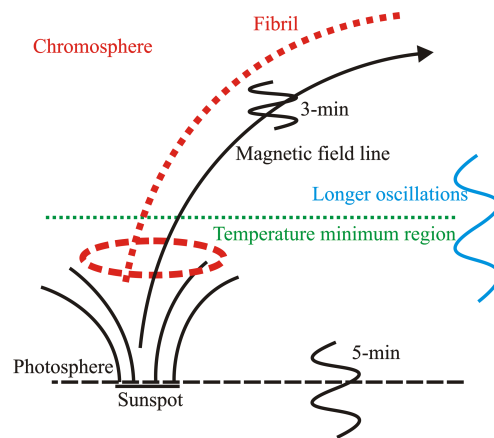


Fig. 13 An illustration depicting the interaction between the chromosphere, photosphere and the role of the fibril in connecting different layers.

In particular, for the long period of 15 minutes in the blue wing of $H\alpha$, this area might play a role of the pass filter for frequency, as well as the magnetic-field interaction. It is very likely that in the same region, the fibril also formed due to the filtering process just below the temperature minimum region. It explains how there is transparency in the temperature minimum region. At the same time, the fibril was also loading the material from below, which was brought by the magnetic field before it flowed from below the chromosphere (just above the red circle after departing from the temperature minimum region in Figure 13). We believe that it might be able to add to the picture of de la Cruz Rodríguez & Socas-Navarro (2011), that chromospheric fibrils are a visual proxy for the magnetic field lines and may need to be reconsidered. This does not necessarily mean that there might be a different mechanism, but there might be a filtering process operating in the magnetic field along the fibrillar pattern.

4.1 LB Connection?

In Figure 6, for both the 2nd column in $H\alpha$, the line center and blue wing (3rd and 2nd rows), we observed a lane-like structure that looked like an LB structure.

The structure can be identified from the average picture on G -band and Ca II H (1st column, 4th and 3rd rows). Is the brightening in 15 minute oscillations also related to the LB? Louis et al. (2008) suggested that the LB could be the sites for heating the overlying chromosphere, based on the low-altitude reconnection, which can be seen as the brightening in the Ca images from a Hinode observation.

We propose that if the LB plays a role in the process, the mechanism would be that LB is the reconnection place (red ellipse in Fig. 13) which is brighter in 3 minute oscillations and the fibril is the ejected material due to reconnection. This argument has a basis in that even though there were no significant activities observed in the Ca II H and G -band, surges that are observed in $H\alpha$ with the LB strengthened in the 3 minute oscillations and the 15 minute oscillations signify the significance of the fibril.

Is this also related to the umbral flash? The enhancement of the Doppler signal in the 3 minute oscillations indicates an enhancement of the chromospheric line of $H\alpha$, but the dynamics in the fibril area do not necessarily define the dynamics of all the umbrae.

5 CONCLUSIONS

We have investigated the chromospheric dynamics and how they are related to the photosphere by studying the fibril with high resolution in spatial and temporal observations. The filtering processes in the photospheric region, particularly near the strong magnetic source and its inclination, as well as mass motion flow, can trace the formation process that connects the layers. We have found that (1) the intermittent ejected material through the fibril from Doppler images has clearly shown oscillations, as seen in the $H\alpha$ blue wing and Doppler signal images; (2) the oscillations in the umbrae and penumbrae magnetic field lines above the photosphere cause a gradual broadening and form an area that has a ring shape from 3 to 15 minute oscillations as a function of height. These traced a distinct boundary between the umbrae and penumbrae which suggest there is a comb structure, and indicate that the oscillations could propagate along the inclined magnetic flux tubes from below; (3) the 3 minute oscillations strongly appeared in the inclined penumbrae magnetic field lines and showed a clear boundary for the LB, as seen in the $H\alpha$ line center and $H\alpha$ blue wing; (4) the 5 minute oscillations were dominant in the outer umbrae region near the umbrae-penumbrae boundary, which suggest that the comb structure has a predominantly downward motion; (5) the 7 minute oscillations were transparent in the $H\alpha$ blue wing. However, like the cases of 10 and 15 minute oscillations, they were concentrated in the inner penumbrae, as seen in the $H\alpha$ line center. But is the fibril also related to an umbral flash? From the morphological signature there are indications of an interplay between mass motion and a strong magnetic field, but further analysis is still needed to reveal the interaction between the two.

Acknowledgements The Dutch Open Telescope is operated at the Spanish Observatorio del Roque de los Muchachos of the Instituto de Astrofísica de Canarias.

References

- Beckers, J. M., & Tallant, P. E. 1969, *Sol. Phys.*, 7, 351
- Bogdan, T. J. 2000, *Sol. Phys.*, 192, 373
- Bogdan, T. J., & Judge, P. G. 2006, *Royal Society of London Philosophical Transactions Series A*, 364, 313
- Centeno, R., Collados, M., & Trujillo Bueno, J. 2006, *ApJ*, 640, 1153
- Chae, J., Yang, H., Park, H., et al. 2014, *ApJ*, 789, 108

- de la Cruz Rodríguez, J., & Socas-Navarro, H. 2011, *A&A*, 527, L8
- Handy, B. N., Acton, L. W., Kankelborg, C. C., et al. 1999, *Sol. Phys.*, 187, 229
- Jess, D. B., De Moortel, I., Mathioudakis, M., et al. 2012, *ApJ*, 757, 160
- Krijger, J. M., Rutten, R. J., Lites, B. W., et al. 2001, *A&A*, 379, 1052
- Leenaarts, J., Rutten, R. J., Carlsson, M., & Uitenbroek, H. 2006, *A&A*, 452, L15
- Leighton, R. B., Noyes, R. W., & Simon, G. W. 1962, *ApJ*, 135, 474
- Lites, B. W. 1992, in *NATO Advanced Science Institutes (ASI) Series C*, Vol. 375, *NATO Advanced Science Institutes (ASI) Series C*, ed. J. H. Thomas & N. O. Weiss, 261
- Louis, R. E., Bayanna, A. R., Mathew, S. K., & Venkatakrishnan, P. 2008, *Sol. Phys.*, 252, 43
- McAteer, R. T. J., Gallagher, P. T., Williams, D. R., et al. 2002, *ApJ*, 567, L165
- Nagashima, K., Sekii, T., Kosovichev, A. G., et al. 2007, *PASJ*, 59, 631
- Reznikova, V. E., & Shibasaki, K. 2012, *ApJ*, 756, 35
- Roupe van der Voort, L. H. M., Rutten, R. J., Sütterlin, P., Sloover, P. J., & Krijger, J. M. 2003, *A&A*, 403, 277
- Rutten, R. J. 2006, in *Astronomical Society of the Pacific Conference Series*, Vol. 354, *Solar MHD Theory and Observations: A High Spatial Resolution Perspective*, ed. J. Leibacher, R. F. Stein, & H. Uitenbroek, 276
- Rutten, R. J. 2007, in *Astronomical Society of the Pacific Conference Series*, 368, *The Physics of Chromospheric Plasmas*, eds. P. Heinzel, I. Dorotovič, & R. J. Rutten, 27
- Rutten, R. J. 2012, *Royal Society of London Philosophical Transactions Series A*, 370, 3129
- Rutten, R. J., Hammerschlag, R. H., Bettonvil, F. C. M., Sütterlin, P., & de Wijn, A. G. 2004, *A&A*, 413, 1183
- Schad, T. A., Penn, M. J., & Lin, H. 2013, *ApJ*, 768, 111
- Stangalini, M., Giannattasio, F., Del Moro, D., & Berrilli, F. 2012, *A&A*, 539, L4
- Staude, J. 1999, in *Astronomical Society of the Pacific Conference Series*, 184, *Third Advances in Solar Physics Euroconference: Magnetic Fields and Oscillations*, eds. B. Schmieder, A. Hofmann, & J. Staude, 113
- Vernazza, J. E., Avrett, E. H., & Loeser, R. 1981, *ApJS*, 45, 635
- White, O. R., & Athay, R. G. 1979, *ApJS*, 39, 317